

Thomas B.W.Kirk  
November 14, 1980

## INTRODUCTION

The source for antiprotons for the Tevatron I Project should be as "bright" as possible. Since brightness is connected inversely with emittance and since there is a large angular emittance of the antiprotons due to their production transverse momentum, it is desirable to make the source have the smallest practical spatial size. Two basic considerations limit the spatial dimensions of the source, finite density of real target materials and multiple coulomb scattering in the target itself.

The first effect introduces a "depth of field" optical aberration and the second increases both the angular spread of the source and the effective source size. In practical schemes, the instantaneous and average energy deposition in the target by the proton beam which makes the antiprotons also introduces a "depth of field" optical aberration and the second increases both the angular spread of the source and the effective source size. In practical schemes, the instantaneous and average energy disposition in the target by the proton beam which makes the antiprotons also introduce serious (and to some extent separable) constraints on the problem. Finally, the proton beam incident has a finite emittance of its own which has an impact on the result separable to some extent from the target heating problems. Many people have made estimates and analytic formulations of various combinations of the above factors and drawn conclusions of seemingly contradictory nature. Since a complete numerical calculation of the  $\bar{p}$  emittance, including all of the effects in an accurate manner, is possible, it seemed useful to do this calculation and summarize the results for use by optical transport programs concerned with capturing  $\bar{p}$ 's for cooling and storage.

In this study, the target density will be assumed to remain constant since exploding targets will be very unlikely in a practical scheme. It is further clear that the overall production cross section for  $\bar{p}$ 's factors out of the problem and is therefore not addressed explicitly here. The production transverse momentum, on the other hand is a crucial factor, and a model for this is introduced. Likewise, chromatic effects due to finite momentum spread of the  $\bar{p}$ 's is not explicitly carried along, but its effect is presented in one study here.

## INPUT MODELS and DATA

Several elements are assumed in making a study of practical use. Let us

- a) Proton beam: The incident proton beam is assumed to have a symmetric x and y gaussian emittance in x and x' given by

$$\epsilon_y = \epsilon_x \equiv \pi \sigma_x \sigma_{x'} = 0.05 \pi \text{ mm mr. (1 standard deviation)}$$

It is also assumed that the beam size and divergence can be varied within the constraint that phase space(emittance) is conserved.

- b) Target: The target is assumed to be tungsten(but if rhenium is used, its parameters are virtually identical) of transverse size large compared to the beam spot. In particular, all particles are assigned multiple scattering(and nuclear attenuation) as though they cannot escape from the sides of the target.

- c)  $\bar{p}$  Production transverse momentum - the antiprotons are assumed to have a production transverse momentum wrt the proton direction of:

$$\frac{dN}{dP_{\perp}^2} = C_0 e^{-(P_{\perp x}^2 + P_{\perp y}^2)/2\sigma_{\perp}^2}, \sigma_{\perp} = 0.40(\text{GeV}/c).$$

- d) Target length: Target lengths of 0.0, 2.0, 4.0, 6.0, 8.0 cm are considered.
- e) Target efficiency: The yield per incident proton per  $\bar{p}$  produced is lowered by attenuation in the target of the incident protons and of the produced  $\bar{p}$ 's. This efficiency factor  $F_{tgt}$  is given by:

$$F_{tgt}(\lambda_p, \lambda_{\bar{p}}, \ell) = \frac{e^{-\ell/\lambda_p} - e^{-\ell/\lambda_{\bar{p}}}}{(\lambda_p/\lambda_{\bar{p}} - 1)},$$

where;  $\ell$  = target length(cm)

$\lambda_p$  = absorbtion length for high energy(nom 80 GeV) protons(cm)

$\lambda_{\bar{p}}$  = collision length for low energy(nom 5 GeV) antiprotons(cm).

note:

if  $\lambda_p = \lambda_{\bar{p}}$ , then,

$$F_{tgt}(\lambda, \ell) = \frac{e^{-\ell/\lambda}}{\lambda/\ell}.$$

We choose  $\lambda_p \approx 10 \text{ cm}$ ,  $5 < \lambda_{\bar{p}} < 10 \text{ cm}$ .

- f) Multiple scattering: The projected multiple scattering in a "thick" target is a correlated two dimensional gaussian in position and slope, and is given by:

$$\frac{d^2P(\rho, x', t)}{dx dx'} = C_0 e^{-B(x'^2 - 3x'\rho + 3\rho^2)}$$

where;

$x'$  = change in slope(angle) due to multiple scattering in a distance  $t$

$\rho \equiv (x/t)$  = change in transverse position  $x$  from the unscattered orbit by traversing a thickness  $t$  of multiple scattering material

$$B \equiv 4 \left( \frac{\beta P}{E_S} \right) \left( \frac{x_0}{t} \right)$$

$$E_S = .021 \text{ (GeV)}$$

$P, E$  = particle momentum(GeV/c), total energy(GeV)

$\beta \equiv P/E$  = Lorentz velocity parameter

$x_0$  = radiation length of scatterer(cm)

$x_0$  = 0.35 cm (tungsten), 155.0cm(lithium)

$t$  = thickness of scatterer (cm)

$$C_0 = \frac{2\sqrt{3}}{\pi} \frac{x_0 (\beta P)^2}{t^2 (E_S^2)} = \text{normalization constant.}$$

When applying multiple scattering to an optical system, the position/angle correlation must be explicitly acknowledged or erroneous results may be obtained. The spatial multiple scattering distribution accurately factors into the product of the projected multiple scattering in the two perpendicular directions for small angle trajectories(the case at hand).

- g) Lithium lens: The antiproton beam emerges from the production target at 5.35 GeV/c momentum and with relatively large transverse momentum in the current Tevatron I plan. To capture a large fraction of these  $\bar{p}$ 's, a monopole lens made from lithium carrying a large pulsed current is proposed. The multiple scattering and nuclear attenuation in the lens is of interest, so its effects have been included. We describe the lens by:

$L = \text{length} = 10.0 \text{ cm}$

$G = \text{magnetic gradient} = 100.0 \text{ KG/cm}$

With these elements, we can monte-carlo the emittance of the  $\bar{p}$ 's. The method is to choose 10,000 rays from a gaussian proton beam phase space in  $x$  and  $x'$ , assume a  $\bar{p}$  produced uniformly along a target of length  $T$  with a projected transverse momentum chosen according to an gaussian distribution in  $P_{\perp}$  as in c), and propagate this ray with multiple scattering through the remaining target, across a 20.0 cm drift space(measured from the center of the production target) and on through the lithium lens(also with multiple scattering). From this point, the ray can be propagated forward to the focus of the lithium lens or backward (without scattering) to the center of the production target. In both these locations, the thin target phase ellipse in  $(x, x')$  is erect and the one dimensional distributions for a thin target slice are simple.

The actual distributions are not simple for targets of length several centimeters due to depth of field distortions. That, of course, is the whole reason for doing the problem numerically!

## RESULTS

The most direct way to present the results of the monte-carlo calculation is in the form of a density plot of numbers of  $\bar{p}$ 's in small bins of  $x$  and  $x'$ , the transverse position and slope of  $\bar{p}$  rays from the production target. As noted above, all rays are presented as they reproject to the center of the production target. In some cases, the detailed distribution at the "hot spot" near  $x = 0.0$ ,  $x' = 0.0$  is presented in a second plot with finer bin size.

In each of the plots in Figures 2-19, the numbers shown in each bin in the  $(x, x')$  plot represent those particles out of a sample of 10,000 produced  $\bar{p}$ 's that ended up in a particular piece of phase space. Note that this is a two dimensional study in one transverse coordinate, hence the yields into a three dimensional solid angle go as this projected result squared only for small solid angles. Since real beam transports will find it hard to subtend large parts of the phase space, the projected results are nevertheless useful.

The plots labeled "Correlation Plot No.3" have bins of 0.04 cm in  $x$  and 10.0 milliradians in  $x'$ . The border around the central 400 bins

gives the overflow events that do not fit into the scale of the plot. The bottom row and rightmost column give the sums of their respective columns and rows, respectively. The plots labeled "Correlation Plot 4" give the same results in a magnified central region with x bins of 0.02 cm and x' bins of 4.0 mr. The parameters of beam, target and Li lens are included on the plot. Multiple scattering in the target and lens are included unless noted otherwise.

Figure 1 shows the geometry of the problem and Table I summarizes the cases plotted in Figures 2-17.

TABLE I  
Correlation Plots for  $\bar{p}$  Production  
in Tungsten Targets

Figure Number	Beam RMS Width (mm)	Beam RMS Slope (mr)	Target Length(cm)	Target Multiple Scattering	Li Lens Multiple Scattering	Comments
2	0.300	0.167	0.0	YES	YES	Target length study with all multiple scattering and "large" incident proton beam
3	"	"	0.0	"	"	
4	"	"	2.0	"	"	
5	"	"	4.0	"	"	
6	"	"	4.0	"	"	
7	"	"	6.0	"	"	
8	"	"	8.0	"	"	
9	"	"	8.0	"	"	
10	0.075	0.067	4.0	"	"	"Small" beam study with full multiple scattering
11	"	"	4.0	"	"	
12	0.0	0.0	0.0	NO	NO	Phase space for point $\bar{p}$ source
13	"	"	0.0	"	"	Finite target length effect
14	"	"	4.0	"	"	
15	"	"	4.0	"	"	
16	"	"	0.0	"	YES	Effect of multiple scattering in LiLens
17	"	"	0.0	"	YES	
18	0.300	0.167	4.0	YES	YES	$\Delta P/P = \pm 2\%$ added to show chromatic behavior
19	"	"	4.0	"	"	

## INTERPRETATION

The raw phase space density data contained in the plots of Table I can be presented in a number of useful ways. Before combining the effects of beam attenuation in the (finite) target with attenuation of the produced  $\bar{p}$ 's in the same target, it is useful to study the effects of proton beam radius and target length normalized to the same number of  $\bar{p}$ 's emerging from the target. Later, the various attenuation and production factors can be multiplied by the densities to get the actual production members. In all cases we study, the full multiple scattering of the target and lithium lens is included.

In Figure 20, the phase space density of the "hot spot" at  $x = 0.0$ ,  $x' = 0.0$  is plotted versus target length for several incident proton beam radii. The central brightness varies weakly with target length over the range 0-8.0 cm. Likewise, there is a gentle dependence on proton beam radius for radii in the range 0-0.30 mm.

This latter result is seen more clearly in Figure 21 where the central density is plotted versus rms beam radius for several target lengths. Note that the beam phase space density is held constant for each beam radius as is necessary for any real beam focussing system. The phase space density of the incident proton beam is assumed to be  $0.05 \pi \text{ mm mr}$  as noted above. The central phase space density is a concept of limited usefulness. It is primarily valuable for small  $\bar{p}$  phase space acceptances, in which circumstances the yield into an acceptance  $\epsilon_x \epsilon_y$  is given by:

$$\begin{aligned} Y &\approx \left. \frac{d^2 N}{dx dx'} \right|_0 \epsilon_x \epsilon_y \\ &= \int_{-y}^{+y} \int_{-y'}^{+y'} \int_{-x}^{+x} \int_{-x'}^{+x'} dx dx' dy dy' \frac{d^4 N}{dx dx' dy dy'} \end{aligned}$$

For finite solid angle acceptance of  $\bar{p}$ 's, the numerical integral over discrete regions of phase space is more useful. In the case of Figures 2-19, this integral is proportional to the sum over the desired ranges of  $x$  and  $x'$ . In the limit where multiple Coulomb scattering and  $\bar{p}$  transverse momentum are both gaussian in the transverse spatial directions (a good approximation for all cases of practical interest), the full four dimensional phase acceptance goes as the product of the  $(x, x')$  and  $(y, y')$  projections. This being the case, each count in a correlation plot bin represents  $1.0 \times 10^{-4}$  of the  $\bar{p}$ 's produced in the target.

Figure 22 shows the fractional yields as a function of  $\epsilon_x$  for symmetric  $(x, x')$ ,  $(y, y')$  values of the  $\bar{p}$  emittance. The curves are parametric in target length and assume a proton beam of 0.30 mm x 0.167 mr. Full multiple scattering is included; the beam and  $\bar{p}$  attenuation factors are not included at this point. The curves verify the unremarkable fact that large acceptance means efficient collection while small acceptance means small yield. This is not news, but it is useful to see the dramatic increase in  $\bar{p}$  collection as  $\epsilon_x$  varies from  $5\pi$  to say  $50\pi$  mm mr.

Note carefully that the emittance integral is over rectangular regions in  $(x, x')$  phase space rather than the conventional elliptical ones. When comparing these emittances to an acceptance that is elliptical in  $(x, x')$ , but which is nevertheless limited by discrete angular limits, a factor of  $(\pi/4)$  may be needed to obtain the elliptical admittance from the rectangular emittance for fixed angular boundaries.

The effect of finite target length on beam and  $\bar{p}$  attenuation is shown in Figure 23. The best model for proton beam and  $\bar{p}$  attenuation probably lies between the two extreme cases shown. If elastic scattering of protons is ignored (a good assumption) then  $\lambda = 10$  cm. If elastic scattering of  $\bar{p}$ 's is ignored (a questionable, but not unreasonable assumption), then  $\lambda_{\bar{p}} = 10$  cm. If elastically scattered  $\bar{p}$ 's are assumed lost,  $\lambda_{\bar{p}} = 5$  cm. Real life probably lies nearer the  $\lambda_{\bar{p}} = 10$  cm limit.

In Figure 24, the target attenuation factor from Figure 23 multiplies the fractional yields of Figure 22 to produce the actual target length dependent yields in tungsten. To obtain the absolute yield of  $\bar{p}$ 's, it is only necessary to multiply the ordinate shown by the fraction of inelastic proton collisions that produce one or more antiprotons in the accepted  $\bar{p}$  momentum interval. If the momentum acceptance exceeds a few percent, integration of the production over the momentum interval may be necessary.

The  $\bar{p}$  yield is finally the important quantity of interest. It can be given by the equation:

$$N_{\bar{p}} = N_p t f_{TGT} \Delta\sigma \equiv 2\pi N_p \left( \frac{Ed^3\sigma}{dP^3} \right)_0 \sigma_{\perp}^2 \frac{\Delta P_{\parallel}}{E} A(t, \epsilon)$$

where;  $N_{\bar{p}}$  = no. of  $\bar{p}$ 's produced from target  $t$  with mean total energy  $E$ , in the momentum interval  $\Delta P_{\parallel}$ , captured in the symmetric emittance

$$\epsilon_x = \epsilon_y \equiv \epsilon$$

$N_p$  = no. of beam protons incident on the target

$$t = N_o \rho \ell$$

$$N_o = 6.02 \times 10^{23} \text{ (Avagadro's Number)}$$

$\rho$  = density of tungsten (gm/cm<sup>3</sup>)

$\ell$  = target length (cm)

$f_{TGT}$  = finite target length factor (see Figure 23)

$$\Delta\sigma = \int_0^{P_{\perp}^2 \max} \int_{P_{\parallel} \min}^{P_{\parallel} \max} \frac{d^2\sigma}{dP_{\perp}^2 dP_{\parallel}} dP_{\perp}^2 dP_{\parallel} \quad (\text{cm}^2)$$

$E = \bar{p}$  total energy (GeV)

$\Delta P_{\parallel}$  = accepted  $\bar{p}$  momentum bite (GeV/c)

$\sigma_{\perp}^2$  = variance for the assumed  $\bar{p}$  production transverse momentum (assumed gaussian), (GeV/c)<sup>2</sup>

$\left( \frac{Ed^3\sigma}{dP^3} \right)_0$  = invariant per nucleon  $\bar{p}$  production cross section evaluated at  $P_{\perp} = 0$ ,  $E$  (cm<sup>2</sup>/GeV<sup>2</sup>)

$A(t, \epsilon)$  = all the geometrical and target length effects. This is the factor that must be computed numerically. Its value varies from 0 to 1.0; it is dimensionless.

Several of the numbers needed for numerically calculating the  $\bar{p}$  yields are uncertain. The values for  $\sigma_{\perp}^2$  and  $\left( \frac{Ed^3\sigma}{dP^3} \right)_0$  are known only approximately.

Nevertheless, by assuming specific values, we can demonstrate  $\bar{p}$  yields explicitly. The values we choose are given by:

$$N_p = 10^{13}$$

$$\sigma_{\perp}^2 = 0.16 \text{ (GeV/c)}^2$$

$$\left( \frac{Ed^3\sigma}{dP^3} \right)_0 = 1.0 \frac{\text{mb}}{\text{GeV}^2} = \frac{1.0 \times 10^{-27} \text{cm}^2}{\text{GeV}^2} @ E = 5.4 \text{ GeV}$$

$$\Delta P_{\parallel} / E = 0.04$$



With these values, the actual  $\bar{p}$  yields are shown on the right hand scale in Figure 24. From the graph, the emittance and target length dependences are quite clear.

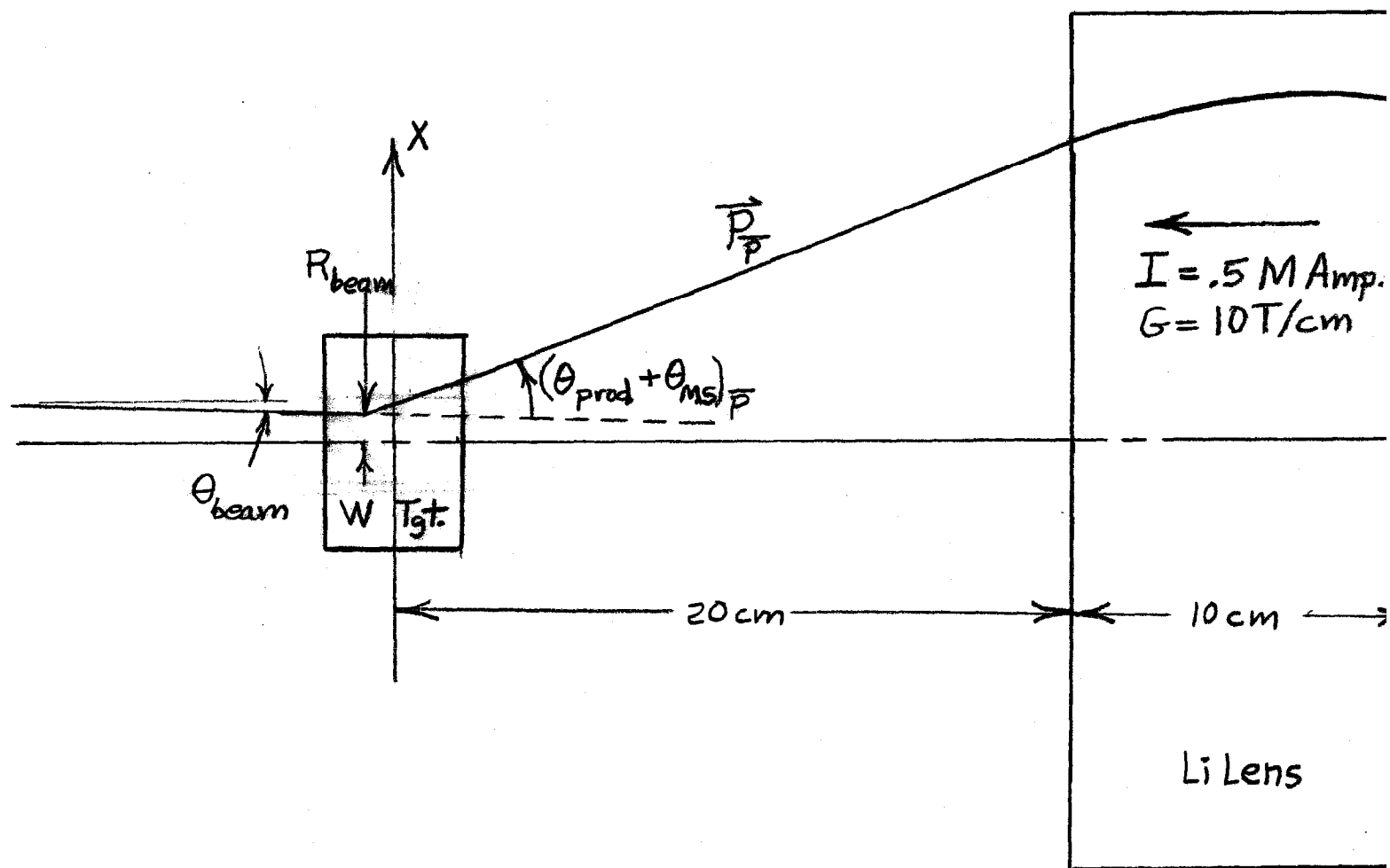


Fig 1  
P Target Geometry

## CORRELATION PLOT NO 3

HORIZ. VARIABLE : DISTANCE FROM AXIS X (CM)

VERTICLE VARIABLE: X SLOPE OF RAY (MILLIRADIANS)

-0.4000

0 0 0 0 0 0 0 0 0 5 45 118 110 29 3 0 0 0 0 0 0

100.0000

0	0	0	0	0	0	0	0	0	1	21	45	65	18	1	0	0	0	0	0	0
00	00	00	00	00	00	00	00	00	2	25	72	60	31	7	00	00	00	00	00	00
00	00	00	00	00	00	00	00	00	4	31	82	95	20	4	00	00	00	00	00	00
00	00	00	00	00	00	00	00	00	7	41	149	134	44	3	00	00	00	00	00	00
00	00	00	00	00	00	00	00	00	9	55	178	150	60	2	00	00	00	00	00	00
00	00	00	00	00	00	00	00	00	10	69	198	184	61	2	00	00	00	00	00	00
00	00	00	00	00	00	00	00	00	13	76	240	230	64	7	00	00	00	00	00	00
00	00	00	00	00	00	00	00	00	14	82	258	260	75	5	00	00	00	00	00	00
00	00	00	00	00	00	00	00	00	15	98	289	265	86	5	00	00	00	00	00	00
00	00	00	00	00	00	00	00	00	16	81	277	241	78	11	00	00	00	00	00	00
00	00	00	00	00	00	00	00	00	17	94	276	243	77	11	00	00	00	00	00	00
00	00	00	00	00	00	00	00	00	18	88	255	270	77	11	00	00	00	00	00	00
00	00	00	00	00	00	00	00	00	19	96	283	252	79	7	00	00	00	00	00	00
00	00	00	00	00	00	00	00	00	20	68	214	238	69	7	00	00	00	00	00	00
00	00	00	00	00	00	00	00	00	21	50	183	193	63	5	00	00	00	00	00	00
00	00	00	00	00	00	00	00	00	22	52	153	172	64	5	00	00	00	00	00	00
00	00	00	00	00	00	00	00	00	23	40	140	130	45	2	00	00	00	00	00	00
00	00	00	00	00	00	00	00	00	24	27	105	98	28	0	00	00	00	00	00	00
00	00	00	00	00	00	00	00	00	25	24	84	84	20	0	00	00	00	00	00	00
00	00	00	00	00	00	00	00	00	26	1	102	93	30	5	00	00	00	00	00	00

-100.0000

0 0 0 0 0 0 0 0 0 1 20 77 65 19 0 0 0 0 0 0 0

SUMMED DISTRIBUTIONS AT BOTTOM AND RIGHTMOST COLUMN

0 0 0 0 0 0 0 0 1 104 1151 3579 3481 1087 104 1 0 0 0 0 0 0

PROTON BEAM RADIUS	=	.0300	CM
PROTON BEAM SLOPE	=	.1557	MILLI RADIANS
TARGET LENGTH	=	0.0000	CM TUNGSTEN
P BAR KINETIC ENERGY	=	4.5000	GEV
P BAR MOMENTUM	=	5.3555	GEV/C
P BAR RMS P PERP	=	.4000	GEV/C
LI LENS GRADIENT	=	100.0000	KG/CM
LI LENS LENGTH	=	10.0000	CM

Full Mult. Scatt.

Fig 2

HORIZ. VARIABLE : DISTANCE FROM AXIS X (CM)

- 2009.

40,000

-40.0000

SUMMED DISTRIBUTIONS AT BOTTOM AND RIGHTMOST COLUMN

0	0	0	0	1	10	49	201	509	887	1276	1241	847	437	192	45	16	0	0	0	0
---	---	---	---	---	----	----	-----	-----	-----	------	------	-----	-----	-----	----	----	---	---	---	---

PROTON BEAM RADIUS	0.0300	CM
PROTON BEAM SLOPE	0.1457	MILLI RADYANS
TARGET LENGTH	0.0000	CM TUNGSTEN
P BAR KINETIC ENERGY	4.5000	GEV
P BAR MOMENTUM	5.3555	GEV/C
P BAR RMS P PERP	0.4000	GEV/C
LI LENS GRADIENT	100.0000	KG/CM
LI LENS LENGTH	10.0000	CM

Full Mult. Scatt.

Fig 3

## CORRELATION PLOT NO 3

HORIZ. VARIABLE : DISTANCE FROM AXIS X (CM)

VERTICLE VARIABLE: X SLOPE OF RAY (MILLIRADIANS)

-0.4000

0 0 0 0 0 1 5 15 21 42 60 49 48 39 15 4 0 0 0 0

100.0000

0	0	0	0	0	0	1	2	18	24	32	31	44	12	5	1	0	0	0	0
00	00	00	00	00	00	00	3	13	41	40	55	48	22	4	0	0	0	0	
00	00	00	00	00	00	00	2	17	55	69	67	57	24	2	0	0	0	0	
00	00	00	00	00	00	00	4	22	60	116	99	55	21	2	0	0	0	0	
00	00	00	00	00	00	00	1	10	79	117	141	70	25	1	0	0	0	0	
00	00	00	00	00	00	00	0	19	76	169	158	80	15	0	0	0	0	0	
00	00	00	00	00	00	00	0	12	92	233	200	79	21	0	0	0	0	0	
00	00	00	00	00	00	00	0	15	80	264	231	58	15	0	0	0	0	0	
00	00	00	00	00	00	00	0	6	90	278	229	83	7	0	0	0	0	0	
00	00	00	00	00	00	00	0	4	83	270	254	73	9	0	0	0	0	0	
00	00	00	00	00	00	00	0	5	74	262	291	88	2	0	0	0	0	0	
00	00	00	00	00	00	00	0	18	83	258	254	100	5	0	0	0	0	0	
00	00	00	00	00	00	00	1	14	79	210	209	93	13	0	0	0	0	0	
00	00	00	00	00	00	00	2	21	97	260	207	83	13	0	0	0	0	0	
00	00	00	00	00	00	00	0	11	76	175	170	84	10	0	0	0	0	0	
00	00	00	00	00	00	00	0	15	66	125	121	75	19	0	0	0	0	0	
00	00	00	00	00	00	00	0	27	64	92	91	55	21	0	0	0	0	0	
00	00	00	00	00	00	00	4	26	54	77	64	43	19	0	0	0	0	0	
00	00	00	00	00	00	00	3	16	44	49	48	45	23	0	0	0	0	0	
0	0	0	0	0	0	0	0	34	38	42	55	39	22	7	1	0	0	0	

-100.0000

0 0 0 0 0 0 2 7 21 34 33 24 33 30 14 3 0 0 0 0

SUMMED DISTRIBUTIONS AT BOTTOM AND RIGHTMOST COLUMN

0 0 0 0 0 0 1 37 334 1355 3084 2986 1355 315 32 2 0 0 0 0

PROTON BEAM RADIUS = .0300 CM  
 PROTON BEAM SLOPE = .1657 MILLI RADIANS  
 TARGET LENGTH = 2.0000 CM TUNGSTEN  
 P BAR KINETIC ENERGY = 4.5000 GEV  
 P BAR MOMENTUM = 5.1355 GEV/C  
 P BAR RMS P PERP = .4000 GEV/C  
 LI LENS GRADIENT = 100.0000 KG/CM  
 LI LENS LENGTH = 10.0000 CM

Full Mult. Scatt.

Fig 4

Full MuH. Scott.

Fig 5



## CORRELATION PLOT NO 3

HORIZ. VARIABLE : DISTANCE FROM AXIS X (CM)

VERTICLE VARIABLE X SLOPE OF RAY (MILLIRADIANS)

-4000

0004-4000

100.0000

[illegible]

00000001

2	7	10	8	15	7	12	9	10	13	17	11	12	7	12	7	11	7	4	3	0
---	---	----	---	----	---	----	---	----	----	----	----	----	---	----	---	----	---	---	---	---

SUMMED DISTRIBUTIONS AT BOTTOM AND RIGHTMOST COLUMN

	9	0	1	5	16	98	206	400	727	1279	1908	1926	1344	693	381	229	120	42	19	5	0	0	9464
--	---	---	---	---	----	----	-----	-----	-----	------	------	------	------	-----	-----	-----	-----	----	----	---	---	---	------

[illegible]

Full Mult. Scatt.

Fig 7



Full Mult. Scatt.

Fig 8

## CORRELATION PLOT NO 4

HORIZ. VARIABLE : DISTANCE FROM AXIS X (CM)

VERTICLE VARIABLE: X SLOPE OF RAY (MILLIRADIANS)

-0.2000

247 118 75 83 73 77 88 87 98 106 98 83 91 109 97 95 93 92 65 57 52

40.0000

0	2	3	13	11	15	23	10	10	11	15	9	14	12	21	15	7	7	3	2	6
00	9	5	3	6	22	17	24	28	27	19	25	18	13	17	11	11	10	6	4	4
00	1	1	1	10	21	19	21	21	22	34	18	11	18	14	12	7	5	4	3	4
00	0	0	0	6	9	25	25	21	20	40	23	23	15	10	11	5	5	1	3	3
00	0	0	0	2	7	19	21	30	27	25	30	25	15	16	16	5	4	4	1	1
00	0	0	0	1	4	13	25	19	39	41	34	27	20	14	10	6	4	4	0	0
00	0	0	0	1	7	7	25	30	39	47	31	32	24	14	7	6	4	1	0	0
00	0	0	0	1	2	4	21	35	36	44	55	39	25	15	14	7	6	3	3	3
00	0	0	0	1	5	11	12	27	44	45	54	38	40	13	11	7	0	1	1	0
00	0	0	0	1	3	10	17	27	43	53	57	47	21	22	5	3	1	0	0	0
00	0	0	0	1	3	3	14	27	39	39	67	30	30	22	4	2	0	0	0	0
00	0	0	0	1	6	10	10	20	30	34	54	42	32	18	7	1	0	0	0	0
00	0	0	0	3	8	4	16	27	20	36	44	39	35	28	7	2	0	0	0	0
00	0	0	0	6	9	14	17	26	29	34	33	39	34	17	10	4	1	0	0	0
00	0	0	0	5	5	11	17	23	21	31	45	51	25	24	17	10	1	0	0	0
00	0	0	0	13	13	17	15	14	18	28	26	25	23	21	8	8	3	1	0	0
00	0	0	0	9	9	12	13	21	20	20	21	21	27	22	20	11	7	3	2	1
00	0	0	0	4	9	12	10	22	20	25	22	25	19	22	22	12	7	3	2	0
00	0	0	0	11	11	16	16	15	13	16	16	19	22	22	23	11	11	7	1	4
00	0	0	0	10	22	18	31	32	28	38	28	25	35	32	36	23	19	22	13	5

-40.0000

244 127 57 61 66 86 78 76 83 98 83 85 73 82 83 77 91 84 71 69 63

SUMMED DISTRIBUTIONS AT BOTTOM AND RIGHTMOST COLUMN

0 26 44 62 89 185 259 361 475 561 665 693 598 507 376 258 162 102 63 34 29

PROTON BEAM RADIUS	■	0.0333 CM
PROTON BEAM SLOPE	■	0.1657 MILLI RADIANS
TARGET LENGTH	■	8.0000 CM TUNGSTEN
P BAR KINETIC ENERGY	■	4.5000 GEV
P BAR MOMENTUM	■	5.3355 GEV/C
P BAR RMS P PERP	■	0.4000 GEV/C
LI LENS GRADIENT	■	100.0000 KG/CM
LI LENS LENGTH	■	10.0000 CM

Full Mult. Scatt.

Fig 9

Full Mult. Scatt.

## CORRELATION PLOT NO 4

HORIZ. VARIABLE : DISTANCE FROM AXIS X (CM)

VERTICLE VARIABLE: X SLOPE OF RAY (MILLIRADIANS)

-0.2000

13 34 18 37 78 113 166 169 169 196 194 188 184 168 185 140 99 79 41 26 18

40.0000

0	0	0	0	0	2	12	18	28	36	36	32	22	35	19	5	2	0	0	0	0
0	0	0	0	0	0	3	12	32	34	44	42	30	25	18	5	2	0	0	0	0
0	0	0	0	0	0	0	9	34	50	44	36	35	19	10	5	2	0	0	0	0
0	0	0	0	0	0	0	3	25	54	55	53	45	17	11	7	1	0	0	0	0
0	0	0	0	0	0	0	5	19	60	55	52	31	18	11	1	0	0	0	0	0
0	0	0	0	0	0	0	1	15	42	77	58	33	20	5	0	0	0	0	0	0
0	0	0	0	0	0	0	2	17	55	83	80	42	14	5	4	0	0	0	0	0
0	0	0	0	0	0	0	0	13	47	89	74	40	14	1	1	0	0	0	0	0
0	0	0	0	0	0	0	1	7	40	102	104	43	12	1	1	0	0	0	0	0
0	0	0	0	0	0	0	3	9	34	81	93	37	4	0	0	0	0	0	0	0
0	0	0	0	0	0	0	4	12	49	85	106	57	10	0	0	0	0	0	0	0
0	0	0	0	0	0	0	4	18	44	80	94	54	19	1	0	0	0	0	0	0
0	0	0	0	0	0	1	4	21	49	67	83	57	12	0	0	0	0	0	0	0
0	0	0	0	0	0	2	4	13	53	55	50	46	9	5	0	0	0	0	0	0
0	0	0	0	0	0	4	9	29	35	44	53	47	28	10	0	0	0	0	0	0
0	0	0	0	0	0	0	13	19	31	45	57	47	36	10	0	0	0	0	0	0
0	0	0	0	0	0	11	13	30	30	52	50	37	42	8	2	0	0	0	0	0
0	0	0	0	0	0	3	16	28	32	35	42	32	33	2	5	0	0	0	0	0
0	0	0	0	0	5	5	22	28	47	58	57	66	52	42	13	3	0	0	0	0

-40.0000

13 29 25 47 75 101 124 131 149 144 153 163 129 144 145 146 106 60 65 24 17

SUMMED DISTRIBUTIONS AT BOTTOM AND RIGHTMOST COLUMN

0 0 0 1 7 11 64 164 444 886 1259 1294 837 429 186 50 10 1 0 0 0

PROTON BEAM RADIUS : .0075 CM  
 PROTON BEAM SLOPE : .6667 MILLI RADIANS  
 TARGET LENGTH : 4.0000 CM TUNGSTEN  
 P BAR KINETIC ENERGY : 2.5000 GEV  
 P BAR MOMENTUM : 5.3565 GEV/C  
 P BAR RMS P PERP : 1.4000 GEV/C  
 LI LENS GRADIENT : 100.0000 KEV/CM  
 LI LENS LENGTH : 10.0000 CM

Full Mult. Scatt.

Fig 11

## CORRELATION PLOT NO 3

HORIZ. VARIABLE : DISTANCE FROM AXIS X (CM)

VERTICLE VARIABLE: X SLOPE OF PAY (MILLIRADIANS)

- .4000

100.0000

-100.0000

SUMMED DISTRIBUTIONS AT BOTTOM AND RIGHTMOST COLUMN

PROTON BEAM RADIUS	=	.0300 CM
PROTON BEAM SLOPE	=	.1667 MILLI RADIANS
TARGET LENGTH	=	0.0000 CM TUNGSTEN
P BAR KINETIC ENERGY	=	4.5000 GEV
P BAR MOMENTUM	=	5.3565 GEV/C
P BAR RMS P PERP	=	.4000 GEV/C
LI LENS GRADIENT	=	100.0000 KG/CM
LI LENS LENGTH	=	10.0000 CM

No Mult. Scatt.

Fig 12

CORRELATION PLOT NO 4

HORIZ. VARIABLE :	DISTANCE FROM AXIS X (CM)
VEHICLE VARIABLE:	X SLOPE OF RAY (MILLIRADIANS)

[illegible]

SUMMED DISTRIBUTIONS AT BOTTOM AND RIGHTMOST COLUMN

[illegible]

No Mult-Scatt.

Fig 13

No Mult. Scatt.

Fig 14







## CORRELATION PLOT NO 3

HORI7. VARIABLE : DISTANCE FROM AXIS Y (CM)

VERTICLE VARIABLE: X SLOPE OF RAY (MILLIRADIANS)

-0.4000

0 0 0 0 0 0 0 0 0 0 5 153 147 3 0 0 0 0 0 0 0

100.0000

0	0	0	0	0	0	0	0	0	0	4	65	80	5	0	0	0	0	0	0
0	0	0	0	0	0	0	0	0	0	1	99	98	0	0	0	0	0	0	0
0	0	0	0	0	0	0	0	0	0	3	116	122	0	0	0	0	0	0	0
0	0	0	0	0	0	0	0	0	0	7	194	184	0	0	0	0	0	0	0
0	0	0	0	0	0	0	0	0	0	1	211	211	0	0	0	0	0	0	0
0	0	0	0	0	0	0	0	0	0	1	285	222	0	0	0	0	0	0	0
0	0	0	0	0	0	0	0	0	0	1	313	287	0	0	0	0	0	0	0
0	0	0	0	0	0	0	0	0	0	1	343	335	0	0	0	0	0	0	0
0	0	0	0	0	0	0	0	0	0	5	370	353	0	0	0	0	0	0	0
0	0	0	0	0	0	0	0	0	0	7	349	323	1	0	0	0	0	0	0
0	0	0	0	0	0	0	0	0	0	5	365	342	1	0	0	0	0	0	0
0	0	0	0	0	0	0	0	0	0	5	351	347	7	0	0	0	0	0	0
0	0	0	0	0	0	0	0	0	0	12	373	338	6	0	0	0	0	0	0
0	0	0	0	0	0	0	0	0	0	5	275	334	1	0	0	0	0	0	0
0	0	0	0	0	0	0	0	0	0	5	245	269	2	0	0	0	0	0	0
0	0	0	0	0	0	0	0	0	0	5	215	237	5	0	0	0	0	0	0
0	0	0	0	0	0	0	0	0	0	3	170	182	2	0	0	0	0	0	0
0	0	0	0	0	0	0	0	0	0	3	136	121	2	0	0	0	0	0	0
0	0	0	0	0	0	0	0	0	0	1	116	119	4	0	0	0	0	0	0
0	0	0	0	0	0	0	0	0	0	1	119	134	3	0	0	0	0	0	0

-100.0000

0 0 0 0 0 0 0 0 0 0 2 93 85 1 0 0 0 0 0 0 0

SUMMED DISTRIBUTIONS AT BOTTOM AND RIGHTMOST COLUMN

0 0 0 0 0 0 0 0 0 0 108 4697 4598 108 0 0 0 0 0 0 0

PROTON BEAM RADIUS = 0.0000 CM  
 PROTON BEAM SLOPE = 0.0000 MILLI RADIAN  
 TARGET LENGTH = 0.0000 CM TUNGSTEN  
 P BAR KINETIC ENERGY = 4.5000 GEV  
 P BAR MOMENTUM = 5.3565 GEV/C  
 P BAR RMS P PERP = .4000 GEV/C  
 LT LENS GRADIENT = 100.0000 KG/CM  
 LI LENS LENGTH = 10.0000 CM

Mult. Scatt., Li Lens only

Fig 16

Mult. Scatt., Li Lens only

Fig 17

## CORRELATION PLOT NO. 3

HORIZONTAL VARIABLE #	DISTANCE FROM AXIS X (CM)																			
VERTICAL VARIABLE #	X SLOPE OF RAY (MILLIRADIANS)																			
-0.4000	0	0	1	2	3	12	28	26	29	32	35	21	34	23	17	24	16	18	4	0
100.0000	0	0	0	0	0	3	10	23	28	18	14	16	19	14	13	5	5	0	0	0
0	0	0	0	0	0	6	16	16	15	24	35	30	20	19	27	6	2	0	0	0
0	0	0	0	0	0	10	33	33	39	42	33	40	37	30	25	3	3	0	0	0
0	0	0	0	0	0	3	22	25	51	52	62	73	49	45	21	3	1	0	0	0
0	0	0	0	0	0	1	10	5	62	86	117	112	103	40	13	4	0	0	0	0
0	0	0	0	0	0	0	0	1	54	112	167	148	89	37	7	0	0	0	0	0
0	0	0	0	0	0	0	0	0	21	116	223	209	83	35	3	0	0	0	0	0
0	0	0	0	0	0	0	0	0	12	91	233	234	100	20	0	0	0	0	0	0
0	0	0	0	0	0	0	0	0	12	97	264	265	88	9	0	0	0	0	0	0
0	0	0	0	0	0	0	0	0	11	89	253	266	98	14	0	0	0	0	0	0
0	0	0	0	0	0	0	0	0	101	242	267	96	16	16	1	0	0	0	0	0
0	0	0	0	0	0	0	0	0	22	94	181	198	118	23	3	0	0	0	0	0
0	0	0	0	0	0	0	0	0	32	96	127	154	108	33	1	0	0	0	0	0
0	0	0	0	0	0	0	0	0	34	93	84	123	84	47	9	0	0	0	0	0
0	0	0	0	0	0	0	0	0	52	74	85	79	64	46	17	4	0	0	0	0
0	0	0	0	0	0	0	0	0	54	53	47	53	50	48	20	5	0	0	0	0
0	0	0	0	0	0	0	0	0	1	5	39	37	36	35	31	10	0	0	0	0
0	0	0	0	0	0	0	0	0	10	14	15	25	23	23	22	7	4	1	0	0
0	0	0	0	0	2	6	22	21	21	31	28	34	26	27	22	24	6	1	0	0
-100.0000	0	0	0	5	3	14	10	21	12	13	17	17	19	15	13	16	12	4	4	0
SUMMED DISTRIBUTIONS AT BOTTOM AND RIGHTMOST COLUMN	0	0	0	0	3	17	95	249	639	1381	2357	2434	1340	609	254	78	21	2	0	0
PROTON BEAM RADIUS	= .0300 CM																			
PROTON BEAM SLOPE	= .1667 MILLI RADIANS																			
TARGET LENGTH	= 4.0000 CM TUNGSTEN																			
P BAR KINETIC ENERGY	= 4.4696 GEV																			
P BAR MOMENTUM	= 5.3256 GEV/C																			
P BAR RMS P PERP	= .4000 GEV/C																			
LI LENS GRADIENT	= 100.0000 KG/CM																			
LI LENS LENGTH	= 10.0000 CM																			

Full Mult. Scatt.

Fig 18

Fig 19

Fig 20

CENTRAL BRIGHTNESS  
VS

TARGET LENGTH

$E_p = 5.4 \text{ GeV}$

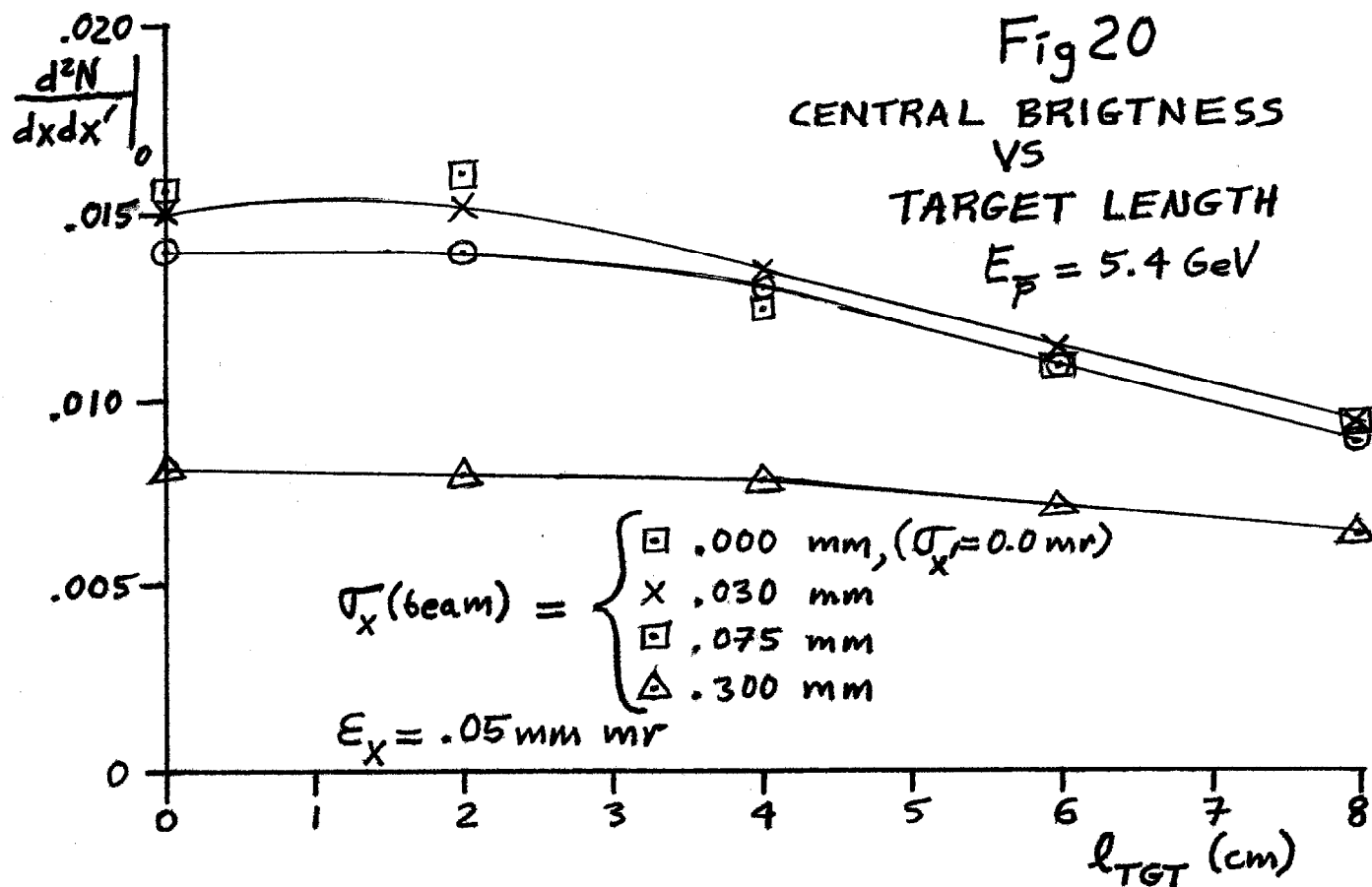
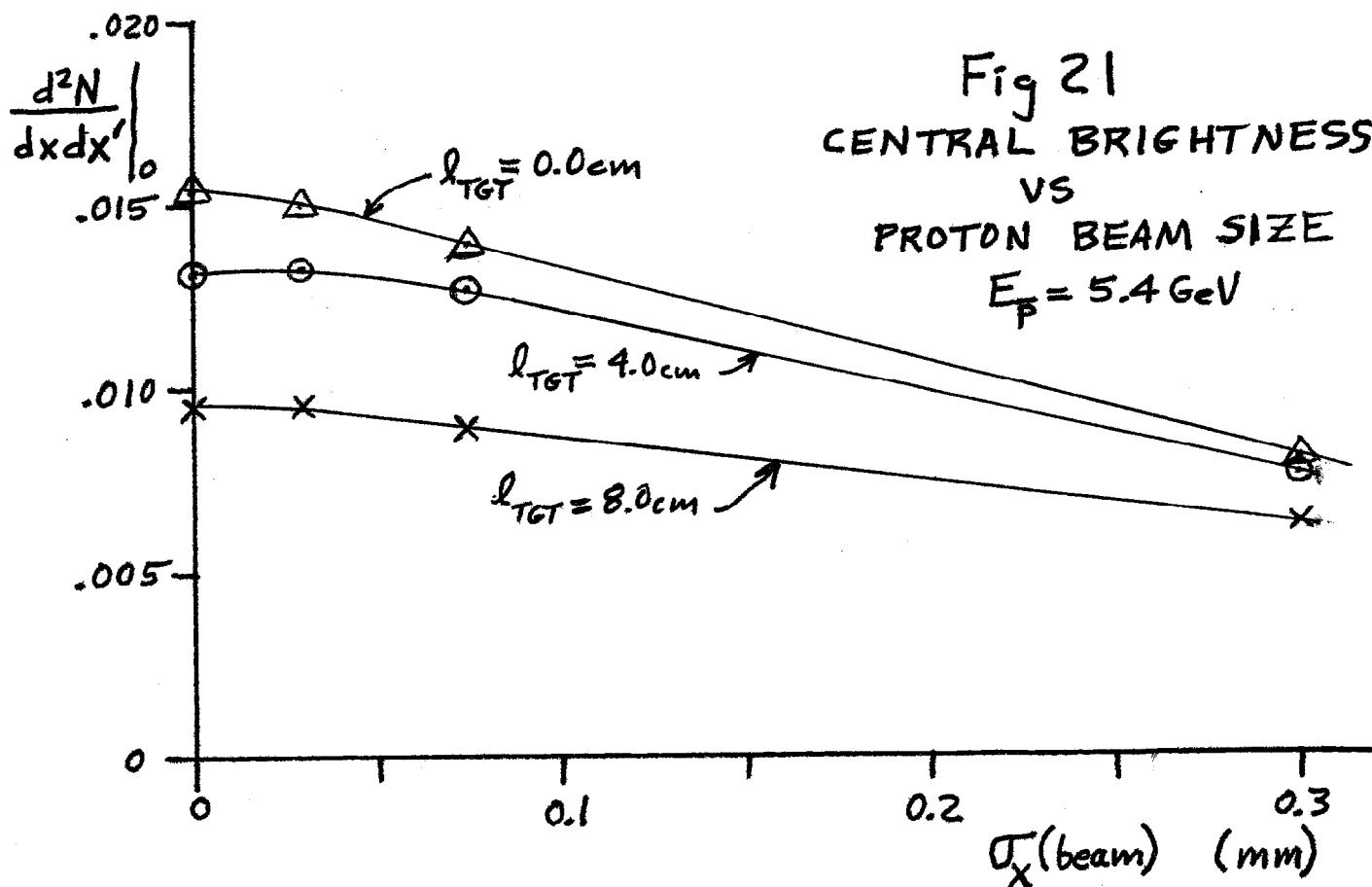


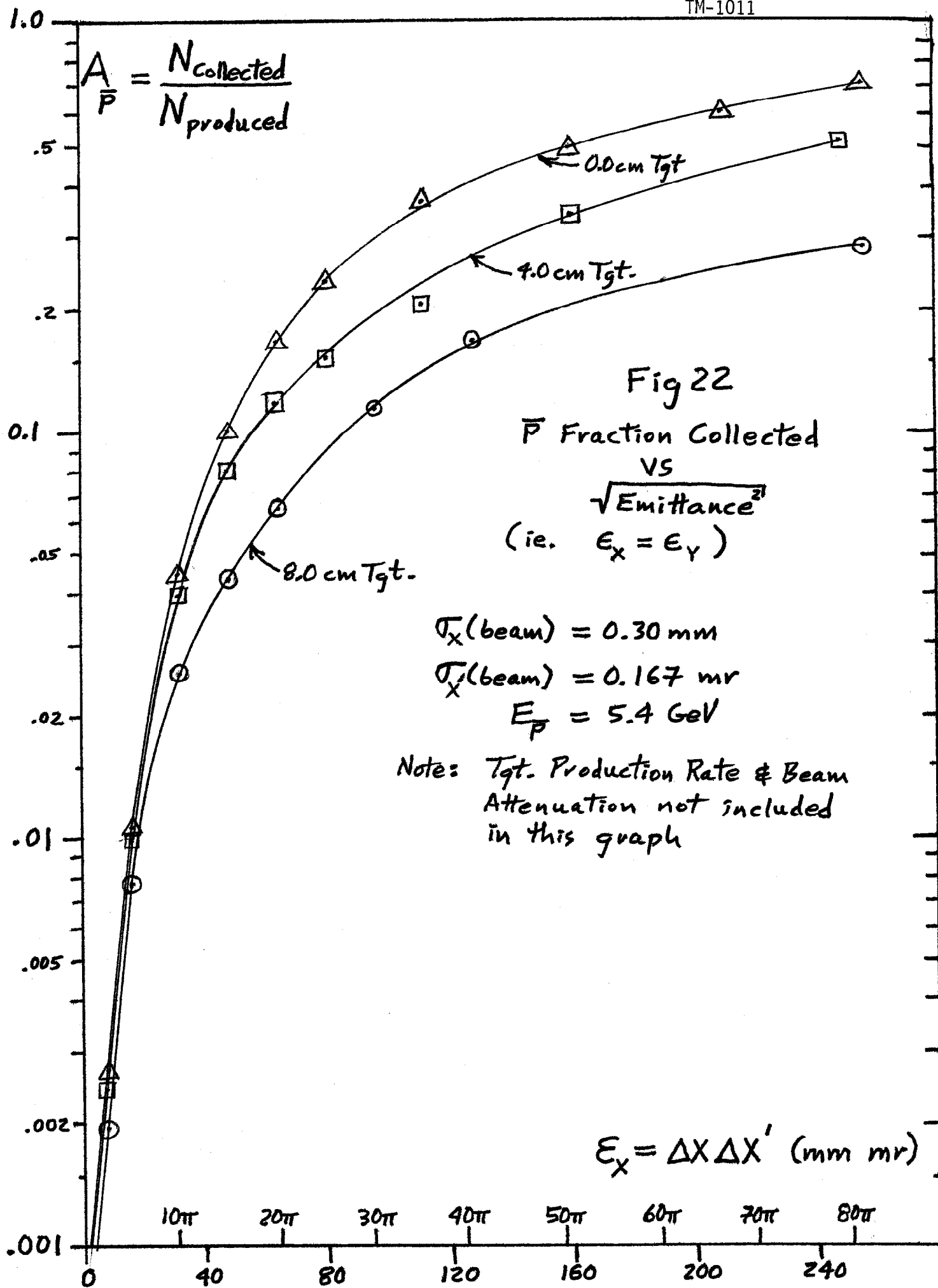
Fig 21

CENTRAL BRIGHTNESS  
VS

PROTON BEAM SIZE

$E_p = 5.4 \text{ GeV}$





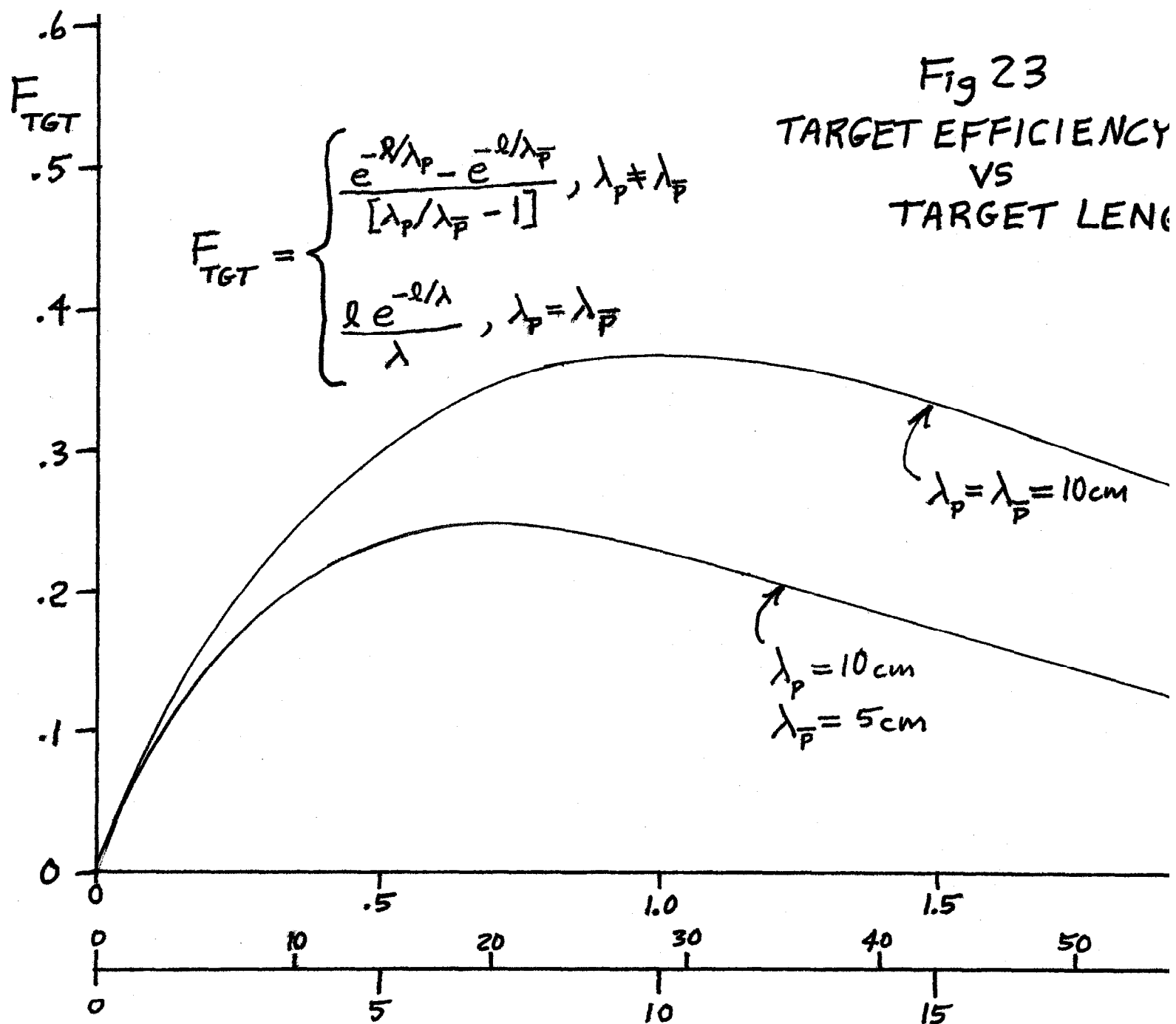


Fig 24

 $\bar{P}$  FRACTIONAL YIELD $\Phi$  $\bar{P}$  FLUX RATE